

Universal Slow Dynamics in Granular Solids

James A. TenCate, Eric Smith, and Robert A. Guyer

Los Alamos National Laboratory, Earth and Environmental Sciences Division, Los Alamos, New Mexico 87545

(Received 27 September 1999; revised manuscript received 22 December 1999)

Experimental properties of a new form of creep dynamics are reported, as manifest in a variety of sandstones, limestone, and concrete. The creep is a recovery behavior, following the sharp drop in elastic modulus induced either by nonlinear acoustic straining or rapid temperature change. The extent of modulus recovery is universally proportional to the logarithm of the time after source discontinuation in all samples studied, over a scaling regime covering at least 10^3 s. Comparison of acoustically and thermally induced creep suggests a single origin based on internal strain, which breaks the symmetry of the inducing source.

PACS numbers: 62.40.+i, 62.65.+k, 91.60.-x

Relaxation processes in which some stress is relieved as the logarithm of time after a step function is applied are remarkably common: in mechanical response of rocks [1] and metals [2], thermoremanent magnetization relaxation in spin glasses [3], dc susceptibility in granular magnetic media [4], and even fluid invasion percolation in soils [5]. Though these systems have completely unrelated microscopic dynamics, they have in common that these forms of creep all monotonically minimize a free energy in response to a constant external stimulus, *respecting* the symmetry of the source.

In studies of nonlinear elasticity of many rocks, it was found that, at strains $\sim 10^{-6}$, retarded effects resembling creep appeared, which could not be explained with equilibrium elastic theory, either classical [6] or hysteretic [7]. Their universal feature was a persistent drop in elastic modulus, and increase in material damping, which could be induced by harmonic acoustic stressing, and we have since found also by thermal shocking. After the stress or shock is removed, the material properties recover toward their original values as the logarithm of elapsed time, over a featureless scaling regime lasting hours to days. An important feature of this effect, which we call *slow dynamics*, is that the elastic modulus decreases in response to symmetric stress cycling or temperature change of either sign, thus *violating* the symmetry of the inducing source.

This Letter reports properties of slow dynamic response in a variety of sandstones, limestone, and concrete. A resonance method is used to enhance sensitivity to small shifts in material properties: reduced modulus causes resonant frequency to drop, and increased damping lowers the resonant quality factor Q (defined so that successive cycles of an undriven oscillator decrease in magnitude by $e^{-\pi/Q}$ [8].) The materials studied are sufficiently different that there appears to be no universally shared chemistry, characteristic scale, or microstructure, suggesting that slow dynamics may be an emergent form of creep not seen before.

The symmetry breaking of slow dynamics resembles the quick loss of microscopic contact area, and its subsequent restoration as $\log(\text{time})$, in the slip/stick of a static friction bond [9]. Depending on geometry, however, slip may lead

to irreversible change (damage accumulation) while slow dynamic recovery is (at least macroscopically) perfect, even over hundreds of cycles spanning more than a year. The combined resemblance to stress-relieving creep and bond rupture raises the question of whether slow dynamics may arise from a glasslike state, somehow intermediate between equilibrium elasticity and damage formation.

Creep in all familiar systems [1–5,9] is understood as a result of thermal activation, and even in the absence of a full microscopic understanding of slow dynamics, this leads to a generic prediction of temperature dependence of the susceptibility. Therefore, slow dynamic recovery was measured as a function of temperature as well as sample type and, in one case, humidity. The suspected connection to bond rupture suggests that modulus and damping changes are induced by internal straining. Therefore, the shifts from acoustic driving and thermal shocking were also compared. From the known thermal expansion anisotropy of the underlying grain materials, the comparison shows all slow dynamic effects to be consistent with a single strain-dependent origin.

The experimental method, described in detail in Refs. [10,11], is to drive a suspended cylindrical sample of rock or concrete in the fundamental longitudinal elastic mode (Young's mode), with a piezoelectric force transducer cemented between one end of the sample and a massive backload. Acceleration of the opposite end of the sample is measured with a lightweight accelerometer and processed with a lock-in amplifier referenced to the driving signal. The driving force is a harmonic acoustic wave, incremented through the fundamental resonance frequency of the bar, to produce the frequency-dependent lumped-parameter response function of the resonant bar/backload system. These response functions can currently be processed to resolve shifts in Young's modulus of one part per million of the static value.

Figure 1 shows the amplitude of a typical response function, for frequency incremented several times per second, first upward and then downward through resonance. An elastic system described by an equilibrium equation of state, either single-valued (classical) [6] or multivalued

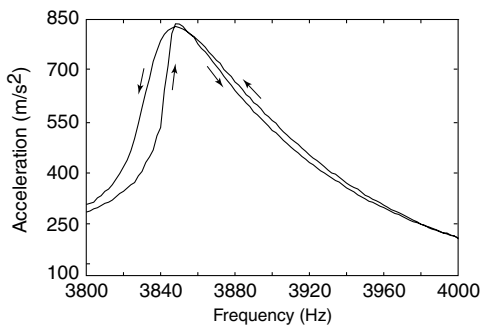


FIG. 1. Partial reproduction of Fig. 2 from Ref. [10]. Amplitude of Young's-mode response of Berea sandstone bar driven at sequence of frequencies, incremented 2 Hz every 300 ms in the direction indicated by arrows. Difference of amplitudes indicates a persistent modulus reduction following periods of high strain, which shifts resonance downward.

(hysteretic) [7], produces an oscillatory strain from harmonic stress, and must have a single-valued amplitude response. The amplitude differences of Fig. 1 are explained if the modulus of the rock drops after periods of high strain, thus moving the effective resonant frequency down for a finite time after each passage through resonance.

The time dependence of the resonant frequency recovery in Fig. 1 was quantified using a two-level force protocol. A high-level driving tone was feedback controlled to track the fundamental resonance for a period of time (usually 15 min) that we call "conditioning." The resonance frequency first drops quickly and then slowly during conditioning, but tracking it with the drive tone ensures that both applied stress and bar strain are constant at known values during this time. The high-level tone is then turned off, and a very low-level tone swept repeatedly through resonance as in Fig. 1. The amplitude and phase of the response are processed as in Ref. [8] to yield the instantaneous resonance frequency and Q over a recovery period of the next hour or more.

Figure 2 shows fractional resonant frequency shift per unit conditioning strain, as a function of time t after the conditioning drive is turned off, for the six samples studied. Lavoux is an oölitic limestone, formed by depositional cementation of oöids, microscopically structure-rich balls grown in seawater by precipitation of supersaturated calcite [12]. Fontainebleau sandstone is formed by silicate cementation of very pure, $\sim 100 \mu\text{m}$ quartz polycrystals with clean surface structure. Berea sandstone is quartz with feldspar and significant interstitial clay, which has both rich topography [13] and complex water chemistry. To provide data on the importance of water, the sample labeled "vacuum" was maintained at elevated temperature in 30 mTorr vacuum for eighteen months prior to and including the experiment; all other samples were kept at room temperature in a dry nitrogen environment, which still permits several percent saturation. Two samples were concrete, one pristine and one damaged by alkali-

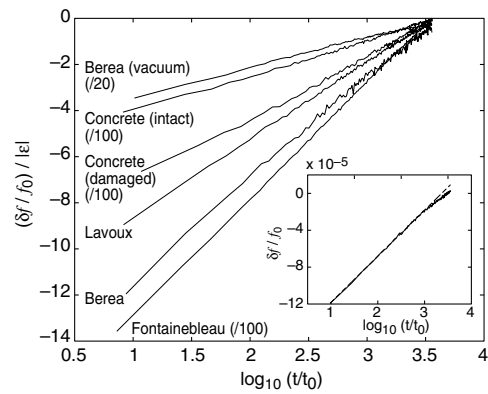


FIG. 2. Time-dependent shift δf of the recovering resonant frequency, normalized by the asymptotic value f_0 , per unit conditioning strain $|\epsilon|$. Sample names are indicated in the figure, and some shifts were scaled by the indicated factors for plotting purposes. The inset is a fit of relative frequency shift, for Berea sandstone in vacuum at 65 °C, to $\ln(t/t_0)$.

silica reaction, which changes the xerogel structure and fluid mobility [14].

The recovery is proportional to $\ln(t/t_0)$ (with t_0 set to 1 s) in all samples, though the sensitivity of the slow-dynamic frequency shift to strain differs by more than 100 between Fontainebleau and Lavoux, with other samples between. Comparison of curves at the same scale in Fig. 2 also shows that all recoveries are not similarly smooth, with the chemically more heterogeneous samples showing more deviation from a perfect logarithm.

Figure 2 (inset) shows a fit of recovering resonant frequency $[\delta f(t) - \delta f(t_0)]/f_0 = m \ln(t/t_0)$, for the vacuum Berea sample at 65 °C. The slope $m = 2.2 \times 10^{-5}$, and apparent breakaway from logarithmic scaling at a time of order 1000 s, characterize this experiment and sample. The breakaway time is somewhat variable, and m depends on conditioning force as well as sample type. [Dependence of the recovery slope on conditioning duration was also measured (not shown), and found to increase in proportion to the maximal total frequency shift attained at the end of the conditioning interval.]

Because creep is expected to be thermally activated, it is useful to introduce a simple model, to understand what features of the energy landscape are constrained by $\log(t)$ recovery. The model we use will attempt to make contact with frictional bond rupture and predicts that, in the absence of finely tuned temperature dependence of the energy landscape, the slope m should scale with temperature. This prediction, together with qualitative expectations about the behavior of Q , is experimentally confirmed below, though not in the simplest form.

Conventional understanding of static friction is that its coefficient μ_s increases in proportion to an actual area of microscopic contact, A_s . In the simplest models, the coefficient of proportionality is a material strength property that may be taken as constant [15]. We will suppose that conditioning results in something equivalent to frictional

slip, and that Young's modulus \mathcal{Y} is also proportional to the microscopic contact area, which contributes parallel stress-transmission paths to those from unruptured or cemented contacts:

$$\mu_s \propto A_s \propto \mathcal{Y}(t) = \mathcal{Y}(t_0)[1 + 2m \ln(t/t_0)]. \quad (1)$$

(A connection between friction and modulus could be checked by extending the experiments of Ref. [15] to measure time dependence of the modulus for shear stress transmission across the bond as it heals.)

Logarithmic area growth should result from formation of bonds impeded by an arbitrary, smooth spectrum of energy barriers [16]. The hopping rate over barriers of energy E is

$$r(E) = \omega_0(E)e^{-E/kT}, \quad (2)$$

where ω_0 is a well-sampling frequency, k is Boltzmann's constant, and T is temperature. If the cleaved area is represented by an initial density of unformed bonds $\rho_0(E)$, the density remaining unformed at time t is

$$\rho_t(E) = \rho_0(E)e^{-r(E)t}. \quad (3)$$

The unrecovered modulus $\delta\mathcal{Y}$ is proportional to the number of unformed bonds:

$$\delta\mathcal{Y}(t) = -\mathcal{Y}_0 \int_{E_1}^{E_2} dE \rho_t(E), \quad (4)$$

where \mathcal{Y}_0 is a reference scale, and E_1 and E_2 are limits on the barrier energies present. As long as the distribution $\rho_0(E)$ is softer than exponential, and the sampled times are well within the limiting rates at E_1 and E_2 , Eqs. (2)–(4) can be approximated as

$$\begin{aligned} \mathcal{Y}(t_2) - \mathcal{Y}(t_1) &\approx \mathcal{Y}_0 \rho_0(E_{\text{char}}) kT \int_0^\infty \frac{dr}{r} (e^{-rt_1} - e^{-rt_2}) \\ &= \mathcal{Y}_0 \rho_0(E_{\text{char}}) kT \ln(t_2/t_1). \end{aligned} \quad (5)$$

E_{char} is a characteristic energy for the times sampled. For the high-temperature assumption $\omega_0 \approx kT/\hbar$, and $10 \text{ s} \leq t \leq 1000 \text{ s}$, $E_{\text{char}} \approx 1 \text{ eV}$.

Careful comparison of the breakaway of Fig. 2 to the equation form (4) is carried out in Ref. [11]. It is clear, though, that the time limit of logarithmic scaling is imposed by $E_2 \approx E_{\text{char}}$ for the relatively narrow range of times sampled here. The energy barriers to slow dynamic recovery are therefore on the scale of crystal defect formation, close-range dislocation interaction [17], or breakage of surfactant bonds.

Since the origin of the supposed spectrum of energy barriers is unknown, there is no reason to assume a particular dependence of $\rho_0(E_{\text{char}})$ on either temperature or time. However, if $\rho_0(E_{\text{char}})$ is weakly temperature dependent, the scaling of the slope for Fig. 2 should lie near the constant- ρ_0 limit of $m = (1/2)\rho_0(E_{\text{char}})kT$. Figure 3 shows the slopes for recovery of the vacuum Berea sample at temperatures in 5°C increments between 30 and 65°C , taken either 12 h or 36 h after incrementing temperature. Temperatures were first decreased and then increased (to screen for progressive damage, which was not found), and

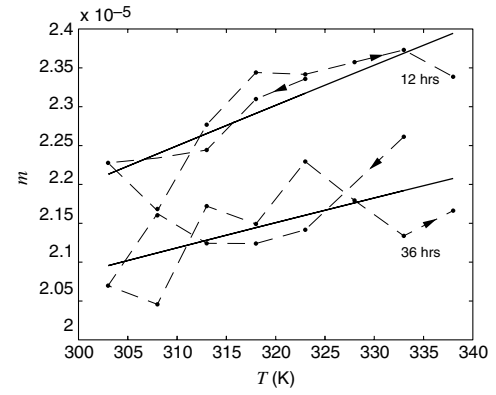


FIG. 3. Slope $m = [\delta f(t) - \delta f(t_0)]/[f_0 \ln(t/t_0)]$, versus temperature, at 12- and 36-h delays after temperature change. Dots are data; dashed lines and arrows indicate temporal order of measurements. Solid lines are power-law fits $m \propto T^{0.7}$ at 12 h, and $m \propto T^{0.5}$ at 36 h.

the temperature range was set by apparatus limitations (low end) and baking thresholds for clays (high end).

Recovery rates are temperature dependent at both times, but neither scales linearly with temperature, and the power law is smaller at 36 h than at 12 h. In terms of Eq. (5), $\rho_0(E_{\text{char}})$, which defines a susceptibility for creep, depends on both temperature and the time delay after it is changed.

The smaller-than-expected scaling of the susceptibility in Fig. 3 may be qualitatively related to the observation that slow-dynamic softening is induced by temperature change itself, independently of oscillatory driving. Figure 4 shows frequency and quality factor shifts from rapid changes between 55 and 60°C . The material softens in both cases, and while the frequency drop is only $\sim 0.1\%$, Q decreases by a remarkable 10% .

A large decrease in Q suggests creation of new multi-stable states with barriers small enough to be activated within an elastic cycle. If this arises from slip, it should be due to the stress field created by anisotropic expansion and random orientation of grains. Stress relaxation by

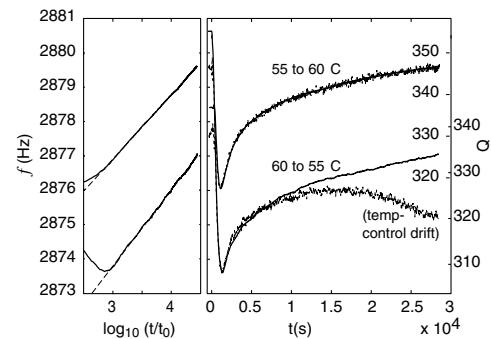


FIG. 4. Resonant frequency (smooth solid curve) and quality factor (noisier dashed curve), after temperature changes $55^\circ\text{C} \rightarrow 60^\circ\text{C}$ and $60^\circ\text{C} \rightarrow 55^\circ\text{C}$. Difference of recovery asymptotes from initial values indicates $t \rightarrow \infty$ equilibrium dependence of sound speed and Q on temperature. Semilog plot of frequencies shown in left-hand panel.

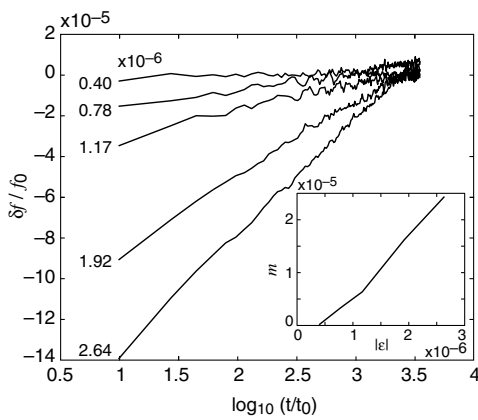


FIG. 5. Dependence of recovery slope on conditioning magnitude. Maximal conditioning strain indicated for individual recoveries $[\delta f(t) - \delta f(t_0)]/f_0 = m \ln(t/t_0)$, and the relation of slope to maximal instantaneous conditioning strain, $m \approx 11.1 \times (|\epsilon| - 4.7 \times 10^{-7})$, is shown inset.

creep restores contact area, reducing the number of low-barrier events available. If the number of higher-barrier events diminishes in kind, $\rho_0(E_{\text{char}})$ will decrease over time, correlated with $1/Q$. Such a correlation, together with the observation that Q increases with temperature, would explain how decreasing ρ_0 compensates the T -linear slope of Eq. (5) to produce Fig. 3. Why this is more visible at 36 h than at 12 h we do not know.

The prediction that modulus reduction results from an induced internal strain field of arbitrary origin can be tested by comparing the magnitudes of acoustically and thermal-shock driven shifts. Figure 5 shows modulus recovery as a function of time at five different acoustic conditioning strains. The relation of the logarithm coefficient to maximal conditioning strain, $m \approx 11.1 \times (|\epsilon| - 4.7 \times 10^{-7})$, is shown (inset).

The acoustic scaling relation can be extrapolated and compared to the thermal recoveries. Under 5°C temperature change, the internal strain of a randomly oriented matrix of quartz crystals may be estimated from the difference of grain parallel- and perpendicular-axis coefficients of expansion, $\delta\alpha \approx 0.65 \times 10^{-5} \text{ }^\circ\text{C}^{-1}$ [18], as $|\epsilon| \sim 3.25 \times 10^{-5}$. The slope then predicted by the Fig. 5 dependence is $m = 3.6 \times 10^{-4}$, close to the fit value $m \approx 2.8 \times 10^{-4}$ from Fig. 4.

Logarithmic scaling persists in Fig. 4 to $\sim 3 \times 10^4$ s, where the acoustic scaling regime ended at $\sim 10^3$ s. In spin glass aging [19], the transition time between logarithmic and power-law scaling is known to depend on the time

between quench and removal of the external induction. If a similar dependence characterizes the dc susceptibility in granular magnetic media [4], it would be interesting to see if they experience a symmetry-breaking susceptibility shift under ac drive, analogous to ours.

This work was supported by the Department of Energy, Office of Basic Energy Sciences, Contract No. W-7405-ENG-36.

-
- [1] N. Carter, *Rev. Geophys. Space Phys.* **14**, 301 (1976).
 - [2] C. Zener, *Elasticity and Anelasticity of Metals* (The University of Chicago Press, Chicago, 1948).
 - [3] K. H. Fischer and J. A. Hertz, *Spin Glasses* (Cambridge University Press, Cambridge, 1991), p. 8.
 - [4] L. J. Swartzendruder, L. H. Bennett, F. Vajda, and E. Della Torre, *Physica (Amsterdam)* **233B**, 324 (1997).
 - [5] D. L. Sparks, *Soil Physical Chemistry* (CRC Press, Boca Raton, FL, 1986).
 - [6] L. D. Landau and E. M. Lifschitz, *Theory of Elasticity* (Pergamon, New York, 1986), 3rd (revised) English ed.
 - [7] K. R. McCall and R. A. Guyer, *J. Geophys. Res.* **99**, 23887 (1994); R. A. Guyer, K. R. McCall, and G. N. Boitnott, *Phys. Rev. Lett.* **74**, 3491 (1995).
 - [8] E. Smith and J. A. TenCate, *Geophys. Res. Lett.* (to be published).
 - [9] F. Heslot, T. Baumberger, B. Perrin, B. Caroli, and C. Caroli, *Phys. Rev. E* **49**, 4973 (1994).
 - [10] J. A. TenCate and T. J. Shankland, *Geophys. Res. Lett.* **23**, 3019 (1996).
 - [11] J. A. TenCate, E. Smith, and R. A. Guyer (to be published).
 - [12] T. Bourbie, O. Coussy, and B. Zinszner, *Acoustics of Porous Media* (Editions Technip, Paris, 1986), pp. 17, 37, 45, and 185; P. A. Scholle, *American Association of Petroleum Geologists Memior 28* (Rogers Litho, Tulsa, 1979), pp. 11, 17, 44, and 113 [ISBN No. 0-89181-304-7].
 - [13] A. P. Radliński, E. Z. Radlińska, M. Agamalian, G. D. Wignall, P. Lindner, and O. G. Randl, *Phys. Rev. Lett.* **82**, 3078 (1999).
 - [14] G. D. Guthrie and J. W. Carey, *Cem. Concr. Res.* **27**, 1407 (1997).
 - [15] X. Jia, C. Caroli, and B. Velicky, *Phys. Rev. Lett.* **82**, 1863 (1999).
 - [16] L. Bocquet, E. Charlaix, S. Ciliberto, and J. Crassous, *Nature (London)* **396**, 735 (1998).
 - [17] J. P. Hirth and J. Lothe, *Theory of Dislocations* (Wiley, New York, 1982), 2nd ed., p. 80.
 - [18] P. Hidnert and H. S. Kridner, in *AIP Handbook* (McGraw Hill, York, PA, 1957), pp. 4–61.
 - [19] Ref. [3], pp. 276, 284–292.